DOI: 10.1002/ejoc.200500558

Synthesis and Photophysical Studies of New Porphyrin–Phthalocyanine Dyads with Hindered Rotation

João P. C. Tomé,[a,b] Ana M. V. M. Pereira,[a] Cristina M. A. Alonso,[a] Maria G. P. M. S. Neves,[a] Augusto C. Tomé,[a] Artur M. S. Silva,[a] José A. S. Cavaleiro,*[a] M. Victoria Martínez-Díaz,[b] Tomás Torres,*[b] G. M. Aminur Rahman,[c] Jeff Ramey,[d] and Dirk M. Guldi*[c]

Keywords: Covalent dyads / Harvesting systems / Photoinduced energy transfer / Phthalocyanines / Porphyrins

A series of novel porphyrin–phthalocyanine (Por-Pc) dyads **1**–**3** have been synthesized by using standard methodologies for unsymmetrically substituted phthalocyanine preparation. These two chromophoric units have been directly linked for the first time, that is, without any spacer, through the β-pyrrolic position of a *meso*-tetraphenylporphyrin, thus allowing a close proximity of the two units in a rigid arrangement. For this, a novel porphyrin–phthalonitrile precursor **4** had to be prepared. The UV/Vis spectra indicate that the basic electronic characteristics of both individual units (i.e., porphyrin and phthalocyanine) are retained in the hybrid Por-Pc molecules. The short Por-Pc separation in dyads **1**–**3** leads to strong excitonic coupling and ultrafast energy transfer (ca. 10^{12} s^{-1}), as determined by femtosecond transient absorption measurements, from the highly energetic ^{1*}(ZnPor) unit to the ^{1*}(ZnPc), which evolves to populate the long-lived ^{3*}(ZnPc) by intersystem crossing. Interestingly, the energy transfer seems to occur more efficiently in dyads **2** and **3**, which have smaller HOMO–LUMO energy gaps.

Introduction

Porphyrins (Por) and phthalocyanines (Pc) have been intensively studied due to their potential applications in a number of scientific areas, namely in medicine,[1,2] in catalysis,[3,4] as materials for advanced technologies,[5–7] and as biomimetic model systems of the primary processes of natural photosynthesis.[8] Both types of macrocycles are ideal photoactive units with outstanding electronic properties, namely strong absorption in the visible region and fine-tunable redox properties, related to their aromatic π-conjugated system. In this regard, many porphyrin- and phthalocyanine-based multicomponent systems in which one of these chromophores is covalently or nonconvalently linked to another electro- or photoactive unit, such as ruthenium–bipyridine complexes, TTF derivatives, quinones, fullerenes, or ferrocene, have been prepared and their mutual electronic interactions studied.[9]

One of the main advantages of using multichromophoric systems is to harvest a wide range of the solar spectrum, which is of general interest for optical and photovoltaic applications. Torres et al. have gained a broad expertise in preparing bichromophoric systems in which either two differently substituted phthalocyanine units[10] or a phthalocyanine and a different phthalocyanine analog, such as hemiporphyrazins[11] or subphthalocyanines,[12] are connected.

Despite the considerable use of individual phthalocyanines, and especially porphyrins, as chromophores, few examples of porphyrin–phthalocyanine (Por-Pc) dyads have been described. In the previous Por-Pc dyads reported,[13,14] different types of spacers have been used to connect the two macrocyclic subunits. It has been established that, in most cases, an efficient photoinduced energy transfer from the porphyrin to the phthalocyanine unit occurs, and also that the degree of excitonic coupling, and therefore the energy-transfer rate, depends strongly on the mutual orientation and distance between the chromophores.

Recently, a Por-Pc dyad in which the two chromophoric units are directly connected, thus dispensing with the need for a spacer, has been reported.[15] Preliminary fluorescence studies confirmed a strong excitonic coupling between the chromophores as a consequence of the short distance be-

[a] Departamento de Química, Universidade de Aveiro, 3810-193 Aveiro, Portugal
Fax: +351-234-370-084
E-mail: jcavaleiro@dq.ua.pt
[b] Departamento de Química Orgánica, Universidad Autónoma de Madrid, 28049 Madrid, Spain
Fax: +34-91-497-3966
E-mail: tomas.torres@uam.es
[c] Institute for Physical Chemistry, Friedrich-Alexander-Universität Erlangen-Nürnberg, 91058 Erlangen, Germany
Fax: +49-9131-852-8307
E-mail: dirk.guldi@chemie.uni-erlangen.de
[d] Radiation Laboratory, University of Notre Dame, Notre Dame, IN 46556, USA
Supporting information for this article is available on the WWW under http://www.eurjoc.org or from the author.

tween them. However, in this particular case, a certain degree of free rotation can be expected due to the linkage of the phthalocyanine unit to the *meso* position of the porphyrin.

We report herein the synthesis of new ZnPor-ZnPc dyads **1**–**3** in which the phthalocyanine moiety is directly bonded to a β-pyrrolic position of a *meso*-tetraphenylporphyrin, thus hindering free rotation through the direct linking bond (see Figure 1) and keeping both chromophores at a very short distance.

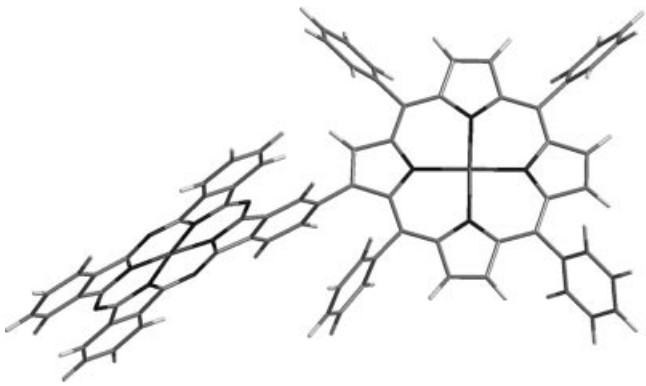

Figure 1. Ball-and-stick representation of ZnPor-ZnPc dyad **1** (PM3 calculations) showing a pseudo-orthogonal arrangement of the Pc unit with respect to the main porphyrin plane.

Dyads **1**–**3** were obtained by statistical crossover condensation of porphyrin–phthalonitrile derivative **4** with different non-porphyrinic phthalonitriles. The synthetic methodology used to prepare the novel porphyrin–phthalonitrile **4** is also described. Different substituents have been introduced in the peripheral position of the phthalocyanine unit in order to evaluate their influence on the photophysical properties of the dyads.

Emission and transient absorption measurements have been carried out to evaluate the excited state Por-Pc interactions in dyads **1**–**3**.

Results and Discussion

Synthesis of the Porphyrin–Phthalonitrile Precursor

The porphyrin–phthalonitrile **4** was obtained in 75% yield by Diels–Alder reaction of diene **5**[16] with fumaronitrile, followed by the oxidation of the resulting adduct **6** with DDQ (Scheme 1). The structure of this new porphyrin–

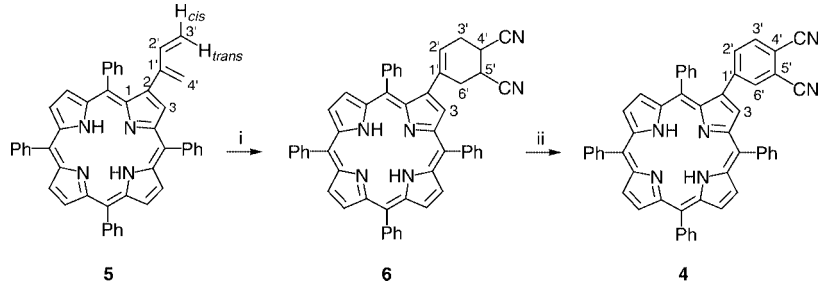

Scheme 1. Synthesis of porphyrin–phthalonitrile **4**. Reagents: i) NCCH=CHCN, toluene, reflux, overnight, 88%; ii) DDQ, toluene, reflux, 24 h, 85%.

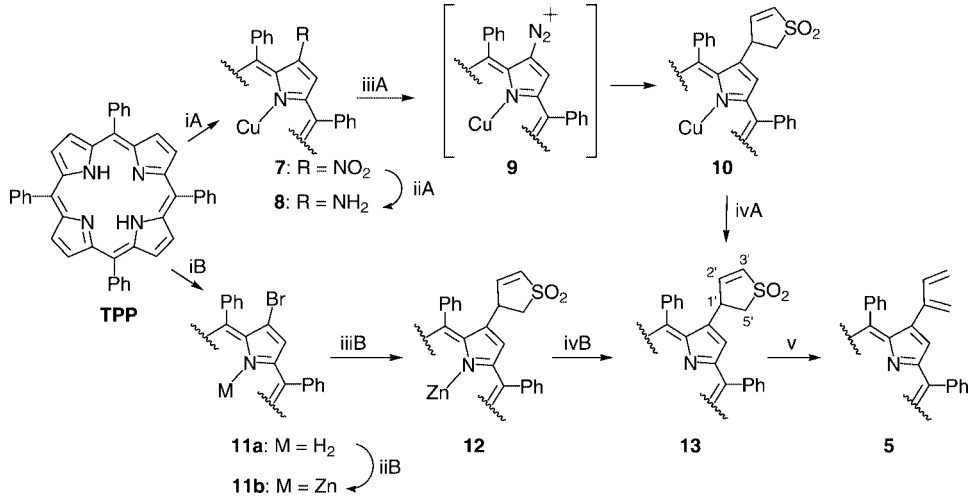

Scheme 2. Synthesis of porphyrin–diene **5**. Reagents: iA) $Cu(NO_3)_2{\cdot}H_2O$, $CHCl_3$, Ac_2O, AcOH, 40 °C, 32 h, 89%; iiA) Sn/HCl, $CHCl_3$, ultrasound, 1 h, 79%; iiiA) first: $NaNO_2$, H_2SO_4, THF/H_2O (1%), 45 min; then: 3-sulfolene, $Pd(OAc)_2$, 65 °C, 81%; ivA) H_2SO_4, $CHCl_3$, 3 min, 92%; iB) NBS, $CHCl_3$, room temp., 6 h, 16%; iiB) $Zn(OAc)_2{\cdot}2H_2O$, $CHCl_3$/MeOH (2:1), reflux, 20 min, 96%; iiiB) 3-sulfolene, $Pd(OAc)_2$, PPh_3, NaOAc, DMF, 24 h, 49%; ivB) TFA, $CHCl_3$, 10 min, 97%; v) DBU, *o*-dichlorobenzene, reflux, 30 min, 87%.

phthalonitrile was unambiguously established from its spectroscopic data, especially ^{1}H and ^{13}C NMR and UV/Vis spectroscopy, and HRMS. The ^{1}H NMR spectrum shows only signals corresponding to aromatic protons, with the characteristic singlet at δ = 8.72 ppm being assigned to the β-proton 3-H resonance.

The porphyrin-diene **5** was prepared by two different routes starting from *meso*-tetraphenylporphyrin (TPP; Scheme 2). oth routes involve a Heck reaction between 3-sulfolene and a TPP derivative (the diazonium salt **9**[16,17] or the 2-bromo-TPP **11b**) in the presence of palladium acetate. The sulfolene derivative **10** was then demetalated to the corresponding free base **13**. The thermal extrusion of SO_2 from **13** gave the expected porphyrinyl butadiene **5** in 87% yield. This reaction was carried out in refluxing *o*-dichlorobenzene in the presence of DBU (required for the isomerization of the 2-sulfolene derivative **13** to the corresponding 3-sulfolene).

Synthesis of Porphyrin–Phthalocyanine Dyads

The ZnPor-ZnPc dyads **1**, **2**, and **3** were prepared by statistical crossover condensation of porphyrin–phthalonitrile **4** with an excess of phthalonitrile, 4,5-dibutoxyphthalonitrile, or 4-*tert*-butylphthalonitrile, respectively, in the presence of zinc chloride as a template (Scheme 3). The reactions were carried out in a refluxing mixture of *o*-dichlorobenzene and *N*,*N*-dimethylaminoethanol (DMAE). As expected, each reaction afforded the desired dyad and the symmetric zinc phthalocyanine formed by self-condensation of the non-porphyrinic phthalonitrile as the main products. During the separation of the reaction mixtures by column chromatography, other minor products were also isolated; their UV/Vis and mass spectra indicate that they are triads of the $(ZnPor)_2$-ZnPc type (see Exp. Sect. and Figure S1 in the Supporting Information).

Structural Characterization of Porphyrin–Phthalocyanine Dyads

Figure 2 shows the UV/Vis spectra of dyads **1**–**3** in THF at the same concentration (3 μM). All three dyads exhibit similar optical features: a broad absorption band at around 344–355 nm, assigned to the Soret band of the phthalocyanine moiety, and a strong absorption band centered at 425 nm due to the Soret band of the porphyrin unit. A strong Q-absorption band at 673 nm (dyad **1**) and at 677 nm (dyads **2** and **3**) is also observed in the spectra.

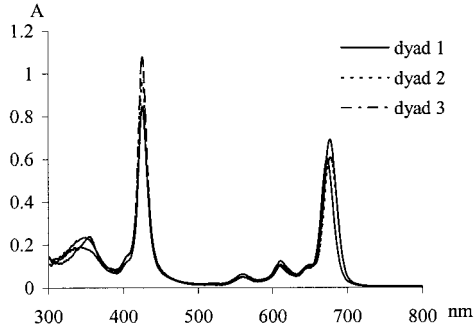

Figure 2. UV/Vis spectra of dyads **1**–**3** in THF (3 μM).

As in previously reported Por-Pc systems,[14a–14c,15] the electronic absorption spectra of all dyads are very similar to those of an equimolar mixture of the corresponding subunits. For instance, Figure 3 compares the UV/Vis spectra of dyad **2** with the spectra of the corresponding porphyrin [ZnTPP, (tetraphenylporphyrinato)zinc(II)] and phthalocyanine [$ZnPc(OBu)_8$, (octabutoxyphthalocyaninato)zinc(II)]. The most remarkable changes are the red shifts observed in all absorption bands (ca. 7 nm) and the smaller absorption coefficients and the broadening of both the porphyrin Soret band and the phthalocyanine Q-band when compared with the parent molecular components. While the small red-shift observed, for instance, in the Pc unit Q-band of dyad **2** in comparison with the phthalocyanine $ZnPc(OBu)_8$ Q-band

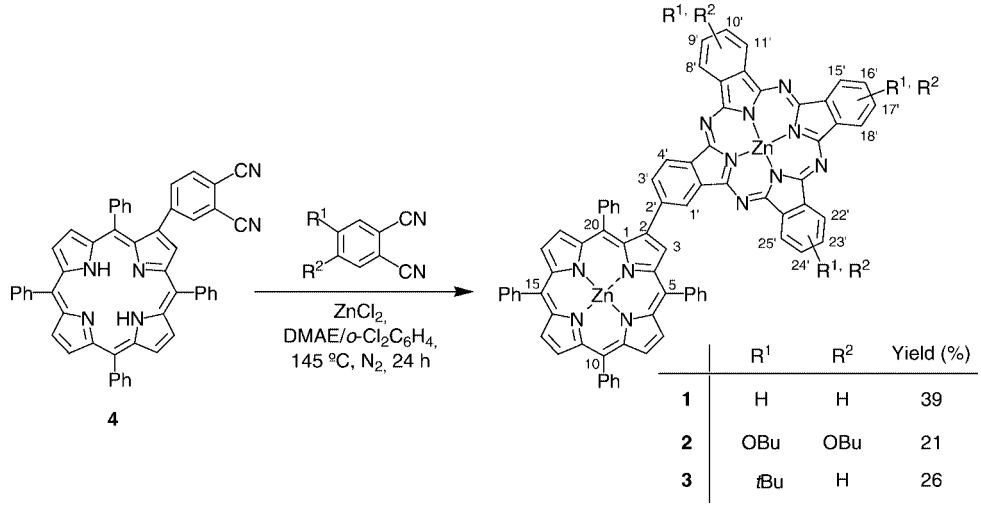

	R^1	R^2	Yield (%)
1	H	H	39
2	OBu	OBu	21
3	*t*Bu	H	26

Scheme 3. Synthesis of the ZnPor-ZnPc dyads **1**–**3**.

can be simply attributed to the different substitution pattern of the two phthalocyanines[18] (two of the butoxy groups of $ZnPc(OBu)_8$ are formally substituted by one porphyrin unit), the smaller absorption coefficients and the broadening of the bands are related to a larger tendency of the dyads to aggregate.

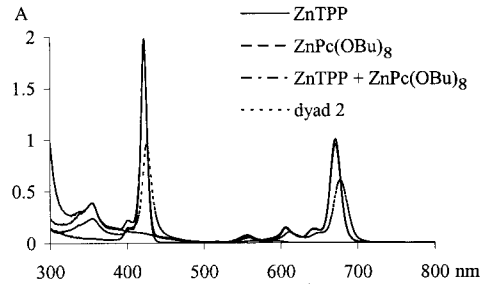

Figure 3. Comparison between the UV/Vis spectra of dyad **2** and those of the corresponding parent porphyrin (ZnTPP) and phthalocyanine [$ZnPc(OBu)_8$] (alone and mixed) in THF (3 μM).

All the new compounds were identified by FAB mass spectrometry and further characterized by HRMS employing the MALDI-TOF technique. In all cases, peaks for the corresponding $[M]^+$ ions were detected.

The NMR studies (^1H, ^{13}C, COSY, HSQC, and HMBC) carried out with dyads **1** and **2** (Figure 4 and Supporting Information) allowed us to identify some of the characteristic protons of the porphyrin and phthalocyanine moieties. However, the ^1H NMR spectrum of dyad **3** gives rise to broad signals irrespective of the solvents and temperatures used, probably due to the fact that this compound is a mixture of positional isomers. The ^1H NMR spectrum of dyad **1** in $CDCl_3$ shows broad signals, which is indicative of intermolecular aggregation. However, a well-resolved spectrum is obtained in $[D_6]$DMSO (Figure S2). In this spectrum we can clearly identify the resonances corresponding to the protons of the porphyrin and phthalocyanine moieties. For instance, the singlet at δ = 9.18 ppm and the signals at δ = 8.70–8.87 ppm are due, respectively, to the resonances of proton 3-H and to the β-protons of the porphyrin moiety. The doublet at δ = 9.05 ppm and the signals at δ = 9.30–9.40 ppm are due, respectively, to the resonances of proton 4′-H and to the remaining α-protons of the phthalocyanine moiety.

On the contrary, the ^1H NMR spectrum of dyad **2** in $[D_6]$DMSO shows broad signals, typical of phthalocyanine aggregation, even when acquired at 50 °C. However, very well "resolved" and sharp NMR signals are observed in the ^1H NMR spectrum of dyad **2** when it is recorded in $CDCl_3$ (Figure 4). Analysis of the ^1H, ^{13}C, and HSQC spectra (Figure S6) allowed the assignment of seven singlets appearing at δ = 8.43, 8.55, 8.90, 8.94, 9.02, 10.37, and 10.53 ppm. The first six singlets correlate, in the HSQC spectrum, with those at δ = 105.36, 105.43, 105.7, 105.8, and 106.2 ppm, and are assigned to phthalocyanine α-proton and carbon resonances. The singlet at δ = 10.53 ppm (3-H) correlates with the carbon signal at δ = 130.4 ppm, and is attributed to the proton and the carbon resonances of the 3-position of the porphyrin moiety.

After the assignment of C-3, and by a careful analysis of the HSQC spectrum, it was possible to assign the other β-carbon resonances of the porphyrin moiety at δ = 129.8, 129.9, 130.0, 131.2, and 131.3 ppm and to identify the region of the β-proton resonances. There is only one β-proton signal outside the aromatic region multiplets, which appears as a doublet (J = 4.6 Hz) at δ = 7.64 ppm.

The ^1H NMR spectrum of dyad **2** also shows three doublets at $\delta \approx$ 10.5 ppm. The multiplicity of these signals (and coupling constants of 7.3, 7.5 and 7.7 Hz) and the correlations found in the COSY (Figure S5) and HSQC spectra allowed us to assign them to the resonances of three *ortho*-protons of three *meso*-phenyl rings of the porphyrin moiety. These data and the correlations found in the COSY spectrum allowed us to conclude that there is no rotation of the *meso*-phenyl rings, since the *ortho*-protons of each phenyl ring are not equivalent. From the ^1H and COSY NMR spectra of dyad **2** we could also identify the proton resonances of the 20-phenyl ring of the porphyrinic moiety at δ = 5.61 (*meta*), 6.00 (*ortho*), 6.07–6.13 (*meta*, *para*), and 8.69 (*ortho*) ppm. The model of dyad **1** depicted in Figure 1 clearly shows the close proximity of this particular *meso*-phenyl ring to the Pc moiety. Consequently, the low frequency values of these resonances are due to the shielding

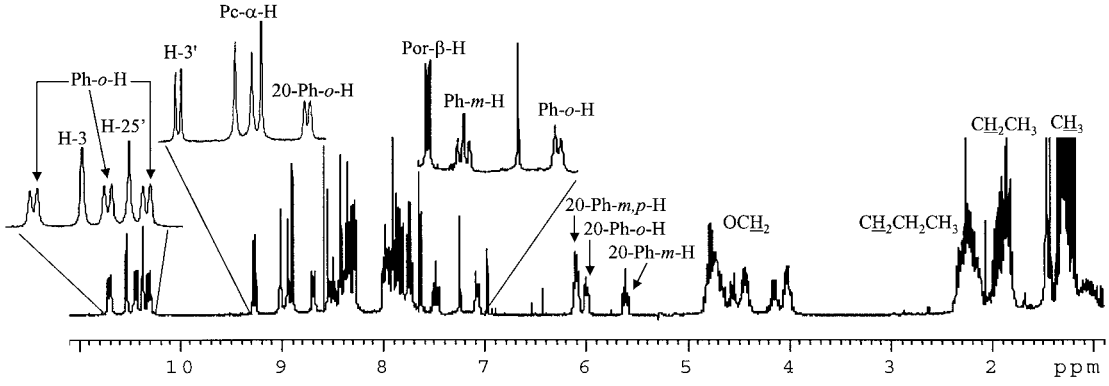

Figure 4. ^1H NMR spectrum of dyad **2** recorded in $CDCl_3$.

effect of the phthalocyanine unit. On the other hand, the absence of free rotation observed for all the *meso*-phenyl rings would be related to intermolecular interactions.

Analysis of the ^{1}H, ^{13}C, COSY, and HSQC spectra of **2** allowed us to assign the multiplets of the aliphatic region to the corresponding methylenic and methyl resonances of the six butoxy groups.

Photophysical Studies of Porphyrin and Phthalocyanine References

To test the excited-state interactions in ZnPor-ZnPc dyads **1**–**3** we first characterized the reference systems ZnTPP [(*meso*-tetraphenylporphyrinato)zinc(II)] and ZnPc*t*Bu$_4$ [(tetra-*tert*-butylphthalocyaninato)zinc(II)] in a series of fluorescence and transient absorption measurements (i.e., steady-state and time-resolved).

Emission and Transient Absorption Measurements

Both references exhibit very high fluorescence quantum yields (see Figure 5 and Table 1). For example, in room-temperature emission experiments (i.e., exclusive excitation of either the Soret- or the Q-band transition) ZnTPP reveals a quantum yield of 0.04. ZnPc*t*Bu$_4$ is an even stronger fluorophore with a quantum yield of 0.3. This renders both probes convenient for the photophysical measurements, especially regarding electronic communication in the target systems **1**–**3**. The fluorescence spectra of ZnTPP and ZnPc*t*Bu$_4$ are in excellent agreement with their mirror-imaged absorption features. The sharp maxima of the *0–0 emission (ZnTPP: $\lambda_{max} \approx 605$ nm; ZnPc*t*Bu$_4$: $\lambda_{max} \approx 700$ nm) differ only slightly from the corresponding 0–*0 absorption, which is indicative of small Stokes shifts. This assignment appears quite plausible as the rigid nature of the π-systems is an important parameter in determining the nuclear coordinates of the excited states relative to those of the ground state. Parallel to the high fluorescence yields, the investigated models show relatively long-lived fluorescence [ZnTPP: 2.0 ns (Figure 7); ZnPc*t*Bu$_4$: 3.1 ns (not shown)].

Next, we performed transient absorption spectroscopy. For example, a 150-fs excitation of ZnTPP in an oxygen-free toluene solution resulted in characteristic absorption changes in the 400–800 nm range (Figure S7). In particular, strong singlet–singlet absorptions are noted in the blue part of the spectrum, that is, between 435 and 500 nm. This feature emerges as an important analytical fingerprint for our work with **1**–**3**. Additionally, a net decrease of the absorption was observed around 540 nm, a region that is, in large, dominated by the ZnTPP ground-state absorption. The net decrease in absorption infers consumption of ZnTPP as a result of converting its singlet ground-state to the corresponding singlet excited state ^{1}*(ZnTPP). A multi-wavelength analysis of the singlet excited state absorption gives rise to a singlet lifetime of 2.5 ns, which is in excellent agreement with previously reported values.[19] The kinetics confirm the lack of appreciable effects that stem from the functionalization of the porphyrin periphery on the singlet excited state properties. Moreover, the singlet lifetime also agrees well with the conclusion of the fluorescence lifetime measurements. For ZnTPP in toluene a fluorescence lifetime of 2.0 ns was determined (see Figure 6).

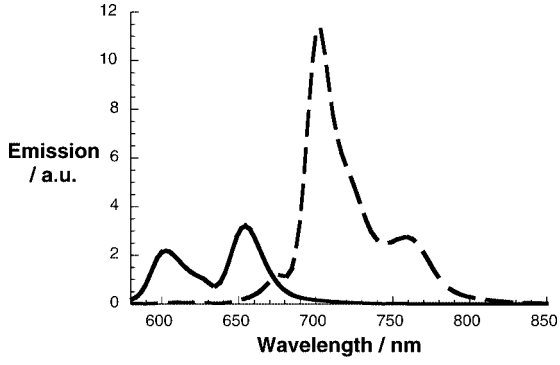

Figure 5. Room-temperature fluorescence spectra of ZnTPP (solid line) and ZnPc*t*Bu$_4$ (dashed line) recorded with toluene solutions that exhibit an optical absorption at the 426-nm excitation wavelength of 0.2.

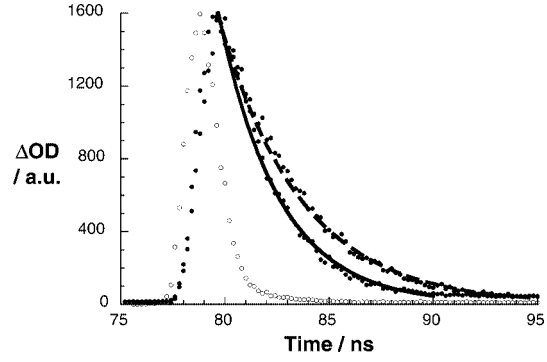

Figure 6. Time-resolved fluorescence decay measurements of ZnTPP at 615 nm (solid line) and ZnPor-ZnPc **1** (dashed line) at 700 nm (excitation wavelength: 337 nm).

Table 1. Fluorescence quantum yields (Φ) and fluorescence lifetimes (τ).

		ZnTPP	ZnPc*t*Bu$_4$	ZnPor-ZnPc (**1**)		ZnPor-ZnPc (**2**)		ZnPor-ZnPc (**3**)	
		Por	Pc	Por	Pc	Por	Pc	Por	Pc
Φ	toluene	0.04	0.3	0.0006	0.21	0.0005	0.18	0.0006	0.18
	THF	0.04	0.3	0.0002	0.19	0.0001	0.2	0.0002	0.2
τ	toluene	1.94	3.1	[a]	3.2	[a]	3.0	[a]	3.0
	THF	1.83	3.2	[a]	3.0	[a]	3.2	[a]	3.0

[a] Outside of our instrumental resolution of 100 ps.

Intersystem crossing (4.0×10^8 s^{-1}) between the singlet ($E_{singlet}$ = 2.00 eV) and triplet manifolds ($E_{triplet}$ = 1.53 eV) is the predominant fate of the photoexcited ZnTPP; the triplet quantum yield in this reference porphyrin is as high as 0.88. Spectral characteristics of the accordingly formed triplet excited-state include a maximum around 860 nm. Again, the derived triplet lifetimes of 44 μs [^{3}*(ZnTPP)] match the values reported previously.[18]

Differential absorption spectra associated with the ZnPc*t*Bu$_4$ reference in an oxygen-free toluene solution show the following features: sharp and very strong minima between 660 and 705 nm and broad but relatively weak maxima between 450 and 600 nm. An illustration is given in Figure 7. The spectral attributes of ^{1}*(ZnPc*t*Bu$_4$), especially the minima, are useful for the mechanistic evaluation of **1**–**3**. On a longer timescale, the singlet excited state ($E_{singlet}$ = 1.79 eV) starts to decay slowly (3.3×10^8 s^{-1}), populating the energetically lower-lying triplet excited state ($E_{triplet}$ = 1.2 eV). Characteristics of ^{3}*(ZnPc*t*Bu$_4$), which is formed with a quantum yield of 0.7, are maxima around 550 nm and minima around 690 nm, similar to those shown in Figure 11.

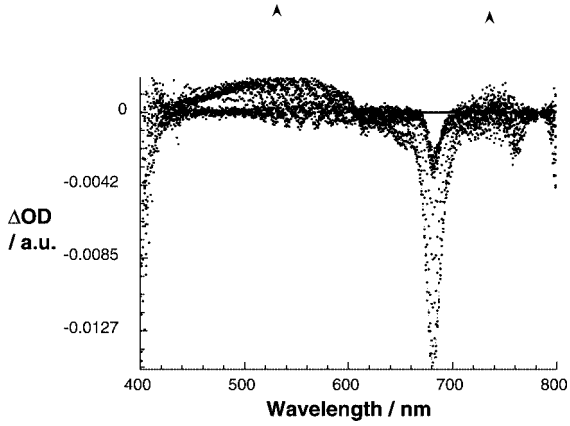

Figure 7. Differential absorption spectrum (visible) obtained upon femtosecond flash photolysis (391 nm) of approx. 1.0×10^{-5} M solutions of ZnPc*t*Bu$_4$ in nitrogen-saturated toluene at room temperature with several time delays between 0 and 50 ps. The spectra correspond to the formation of ^{1}*(ZnPc*t*Bu$_4$).

Photophysical Studies of Porphyrin–Phthalocyanine Dyads

Emission Measurements

Excitation of **1**–**3** either in the spectral region of the ZnPor Soret band (i.e., 426 nm) or the ZnPc Q-band (i.e., 674, 678, 679 nm) allowed the selective probing of the excited-state features of each building block.

Starting with the ZnPor building block, that is, excitation at 426 nm, we found several significant differences with respect to the ZnTPP reference. Firstly, the fluorescence quantum yields were as low as 0.0005 even in nonpolar toluene, and in THF the values are as low as 0.0001. In other words, the ZnPor fluorescence decrease is enhanced more than 100-fold in the presence of ZnPc. Secondly, the familiar ZnPc fluorescence spectrum appears in the near-infrared with a strong *0–0 emission at around 700 nm, despite almost exclusive excitation of the ZnPor moiety at 426 nm. An example is illustrated in Figure 8. Conclusive evidence for the ZnPc emission came from experiments that make use of the heavy-ion effect for a controlled acceleration of the intersystem-crossing process between the ZnPc singlet and triplet manifolds. Addition of ethyl iodide − a heavy-atom provider − led to a complete cancellation of the ZnPc fluorescence.

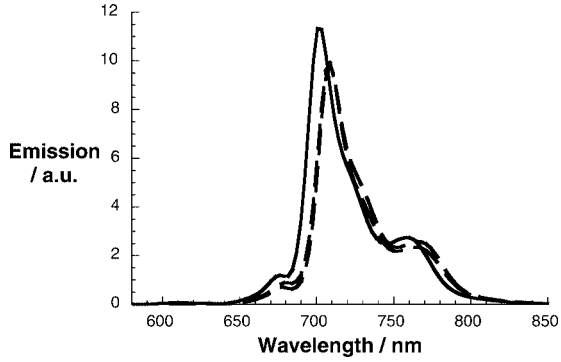

Figure 8. Room-temperature fluorescence spectra of ZnPc*t*Bu$_4$ (solid line) and ZnPor-ZnPc dyads (**1**: dashed line; **2**: dotted line) recorded with toluene solutions that exhibit an optical absorption at the 426-nm excitation wavelength of 0.2.

To unravel, and likewise to test, the mechanism producing the ZnPc emission, a decisive excitation spectrum of the 700-nm emission was taken. In fact, the excitation spectra of dyads **1**–**3** were found to be reasonable matches of those recorded for the ZnTPP reference. Furthermore, the maxima also resemble the ground-state transitions of ZnPor (i.e., Soret and Q-band). Taking this into account we reached the conclusion that the origin of the ZnPc excited state is unquestionably that of ZnPor. Furthermore, this allows us to attribute the underlying mechanism: an efficient intramolecular transfer of singlet excited state energy from the photoexcited ZnPor to the covalently linked ZnPc governs the photophysics of the ZnPor-ZnPc arrays [Equation (1)].

$$\text{ZnPor-ZnPc} \rightarrow {}^1\text{*(ZnPor)-ZnPc} \rightarrow \text{ZnPor-}{}^1\text{*(ZnPc)} \quad (1)$$

The rate constant (k) of the intramolecular singlet–singlet energy transfer in the investigated ZnPor-ZnPc can be calculated from the quantum yields (Φ) of the fluorescence and the lifetime (τ) of photoexcited ZnTPP, according to Equation (2).

$$k = [\Phi_{ZnTPP} - \Phi_{ZnPor\text{-}ZnPc}]/[\tau_{ZnTPP}\ \Phi_{ZnPor\text{-}ZnPc}] \quad (2)$$

The extremely fast rates ($k \approx 10^{11}$ s^{-1}), as determined by Equation (2), infer a strong coupling between the two moieties, a hypothesis that appears reasonable bearing in mind the proximity of the two chromophoric units and their rigid arrangement.

By employing ZnPc*t*Bu$_4$ as a standard, with matching absorption at the excitation wavelength, the ZnPc fluorescence quantum yields were deduced for the different donor–acceptor systems. In toluene, the Φ values nearly approach that measured for the reference ZnPc*t*Bu$_4$, namely 0.3, and

do not vary appreciably with excitation wavelength. It is interesting to note that for the ZnPor-ZnPc arrays the energy transfer appears to occur more efficiently at smaller energy gaps (**2** and **3**), that is, the difference between the singlet excited state of ZnPor and that of ZnPc, than at larger ones (**1**). A possible rationale involves a weaker spectral overlap at larger energy gaps, for instance, between photoexcited ZnPor and ground-state ZnPc.

A different picture emerged upon switching to the ZnPc building block, that is, excitation at around 680 nm. In particular, we found − relative to ZnPc*t*Bu$_4$ − almost no changes at all. The fluorescence quantum yields and fluorescence lifetimes are virtually superimposable with those recorded for ZnPc*t*Bu$_4$ under identical experimental conditions (Figure 6). Tentatively, we conclude that once the singlet excited-state energy is funneled to the ZnPc building block, the photophysical deactivation according to Equation (3) occurs.

$$\text{ZnPor-}^1\text{*(ZnPc)} \rightarrow \text{ZnPor-}^3\text{*(ZnPc)} \rightarrow \text{ZnPor-ZnPc} \quad (3)$$

Finally, we decided to focus on a more polar environment, such as THF. No significant differences were seen, however, relative to the aforementioned data in toluene. This serves as additional proof for an all-energy transfer pathway in photoexcited **1**–**3** [Equation (1)] that is not expected to change notably with solvent polarity.

Transient Absorption Measurements

Since the conclusion of the emission studies presumes that an intramolecular energy transfer prevails, further examination of ZnPor-ZnPc compounds **1**–**3** was deemed necessary.

When comparing Figure 7 and Figure 9, the transient absorption changes observed upon 387-nm laser excitation of the investigated ZnPor-ZnPc arrays are, at first glance, superimposable with those recorded for the ZnPc*t*Bu$_4$ model. (Note that the dominant absorption at the 387-nm excitation is that of the ZnPor moiety in **1**–**3**.) Upon closer inspection, we see evidence for the singlet–singlet characteristics of ZnPor in the 435–500 nm range. The ZnPor fingerprint is, however, unreasonably weak and very short-lived. Both facts speak for an ultrafast deactivation of the photoexcited ZnPor. Generally, similar spectra were noted in toluene and THF for **1**–**3**, regardless of the ZnPc nature and the polarity of the solvent.

In Figure 10 we compare time/absorption profiles at 450 nm and 700 nm, which correspond to spectral regions of ZnPor (i.e., strong singlet–singlet absorption between 435 and 500 nm) and ZnPc fingerprints (i.e., sharp minima between 660 and 705 nm), respectively. Inspection of the 700-nm time/absorption profile shows that the singlet excited-state formation differs in **1**–**3** from what has been seen for ZnPc*t*Bu$_4$. While in ZnPc*t*Bu$_4$ the formation is instantaneous and essentially completed with the conclusion of the short laser pulse, a two-step formation process governs the photophysics of **1**–**3**. Firstly, a rapid formation (i.e., less than 1 ps) is seen that is virtually instantaneous. Secondly, this fast process is followed by a secondary process (i.e., around 1 ps). By fitting the secondary processes to unimolecular rate laws the following rates were determined: **1**: 5.6×10^{11} s^{-1}; **2**: 7.1×10^{11} s^{-1}; **3**: 8.8×10^{11} s^{-1}. Interestingly, as far as rates and efficiencies are concerned we see a similar trend in relation to the steady-state fluorescence measurements. Analysis of the 450-nm time/absorption profiles reveals the ultrarapid deactivation of the ZnPor singlet excited state. Importantly, the decay dynamics of this process match the secondary process of the ZnPc singlet excited state formation.

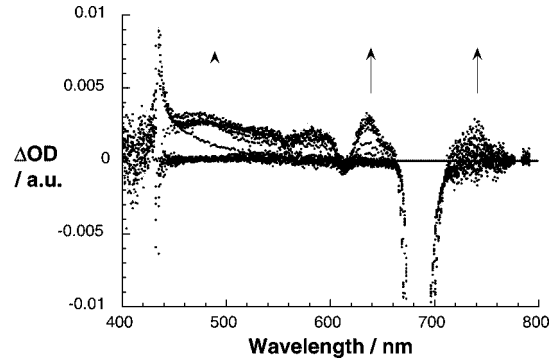

Figure 9. Differential absorption spectrum (visible) obtained upon femtosecond flash photolysis (387 nm) of approx. 1.0×10^{-5} M solutions of **1** in nitrogen-saturated toluene with several time delays between 0 and 50 ps at room temperature. The spectra correspond to the ^{1}*(ZnPc) formation.

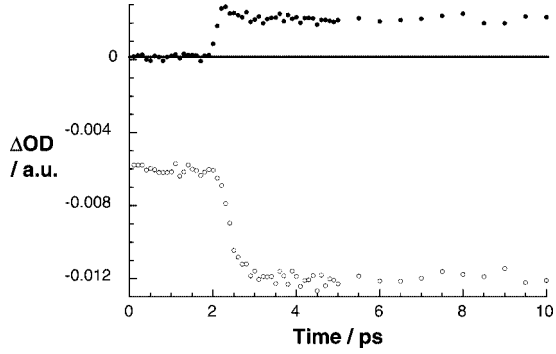

Figure 10. Time-absorption profiles recorded at 450 nm (filled circles) and 700 nm (open circles) for ZnPor-ZnPc (**1**) in deoxygenated toluene solutions. The profiles correlate to the differential absorption changes shown in Figure 9.

Hereafter, an intersystem crossing (i.e., $3.2\pm0.2\times10^8$ s^{-1}) is the predominant deactivation of the ZnPc singlet excited states in **1**–**3**. In line with the proposed energy-transfer mechanism, the only appreciable photoproducts in complementary nanosecond experiments for photoexcited **1**–**3** are those of the ZnPc triplet excited state. Figure 11 illustrates the triplet spectra for **1**–**3**. The lifetimes of the ZnPc triplets were estimated to be around 70 μs. Thus, our analysis clearly shows the photosensitization effect of the ZnPor chromophores, which act as antenna systems and transmit their excited energy to the covalently attached ZnPcs. This enables efficient ZnPc triplet generation, even in a wavelength region where the ZnPc absorption is comparatively weak.

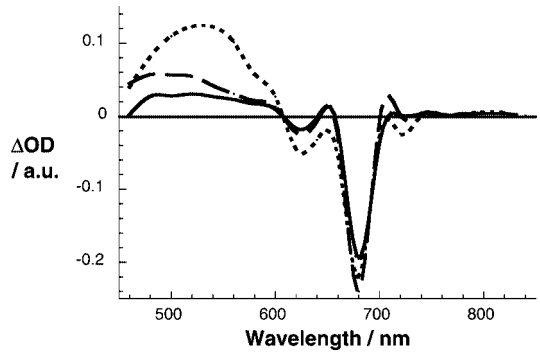

Figure 11. Differential absorption spectrum (visible) obtained upon femtosecond flash photolysis (532 nm) of approx. 1.0×10^{-5} M solutions of **1** (solid line), **2** (dotted line), and **3** (dashed line) in nitrogen-saturated toluene with a 50-μs time delay at room temperature. The spectra correspond to ^{3}*(ZnPc).

To summarize, the short ZnPor-ZnPc separation leads to ultrafast transduction of a singlet excited state with rates of around 10^{12} s^{-1}, as derived from femtosecond transient absorption measurements. Kinetics, on the other hand, which are solely based on the steady-state fluorescence spectra indicate somewhat slower rates, although we believe that these values should only be considered as lower limits due to the extremely strong quenching.

Conclusions

It has been shown that porphyrin–phthalonitrile **4** can be successfully used as a precursor for novel Por-Pc dyads with different substituents on the Pc moiety by employing the classical statistical crossover condensation phthalocyanine synthesis methodology. The porphyrin–phthalocyanine dyads prepared by this method are directly connected through the β-pyrrolic position of the porphyrin unit. The spectroscopic and NMR studies have shown that C–C rotation between the porphyrin and phthalocyanine units is prevented, losing molecular planarity and conjugation. However, the close proximity of the two chromophores allows a strong through-space excitonic coupling between them.

Scheme 4 illustrates the efficient energy transfer, which evolves from the highly energetic ^{1}*(ZnPor) (2.0 eV) to the shallow ^{1}*(ZnPc) (1.79 eV). From there, conventional intersystem-crossing events populate the long-lived ZnPc triplet excited state (1.2 eV). ^{3}*ZnPor is not formed to any appreciable extent, which is mainly due to its unfavorable energetic positioning (1.53 eV) in the ZnPor-ZnPc arrays.

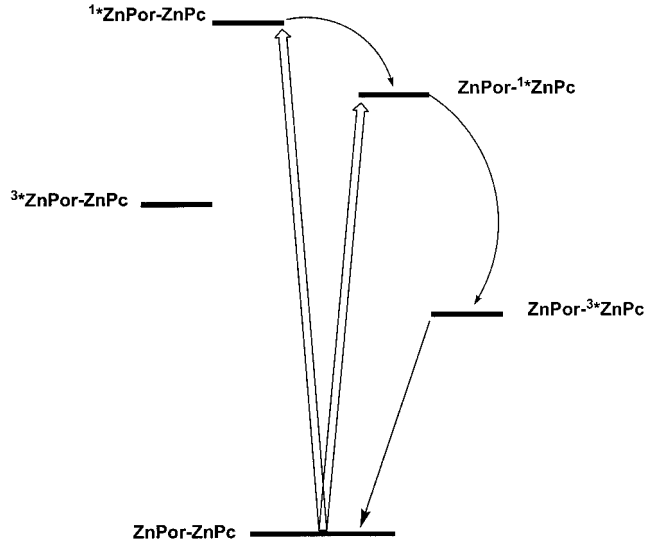

Scheme 4. Photophysical processes in ZnPor-ZnPc dyads.

Experimental Section

General: Solution ^{1}H and ^{13}C NMR spectra were recorded with a Bruker AMX 300 spectrometer at 300.12 and 75.47 MHz, respectively. $CDCl_3$ was used as solvent (except when indicated) and tetramethylsilane as internal reference; the chemical shifts (δ) are expressed in ppm and the coupling constants (J) in Hz. FAB mass spectra were recorded with VG AutoSpec Q and M mass spectrometers using chloroform as solvent and NBA as matrix. HR MALDI-TOF mass spectra were determined with a Bruker Reflex III spectrometer using dithranol as matrix. The UV/Vis spectra were recorded with a Uvikon spectrophotometer using THF as solvent. Melting points were measured with a Reichert Thermovar apparatus fitted with a microscope and are uncorrected. Column chromatography was carried out with silica gel (Merck, 230–400 mesh). Preparative thin-layer chromatography was carried out on 20×20 cm glass plates coated with silica gel (1 mm thick, Merck). Analytical TLC was carried out on precoated sheets with silica gel (0.2 mm thick, Merck).

Porphyrin–Phthalocyanine Dyads 1–3. Typical Procedure: A mixture of porphyrin–phthalonitrile **4** (30 mg, 41 mmol), phthalonitrile (63 mg, 492 mmol), and $ZnCl_2$ (45 mg, 330 mmol) was stirred at 145 °C in a deaerated mixture of *o*-dichlorobenzene and DMAE (1:1) (4 mL) under nitrogen for 24 h. The reaction mixture was precipitated with MeOH/H_2O and the solid was filtered through a short column of Celite, washed with water and MeOH, and then the crude mixture was redissolved in CH_2Cl_2. The desired dyad was separated from the symmetrical phthalocyanine by flash chromatography (silica gel) with a mixture of petroleum ether and THF (4:1). A minor fraction corresponding to triad **1** was also isolated. Dyad **1** was further purified by preparative TLC (silica gel) with a mixture of petroleum ether and THF (4:1). Dyads **2** and **3** were prepared by the same procedure but using 4,5-dibutoxyphthalonitrile or 4-*tert*-butylphthalonitrile, respectively, instead of phthalonitrile. All compounds were crystallized from CH_2Cl_2/petroleum ether.

Dyad 1: Yield: 20 mg (39%); m.p. > 300 °C. ^{1}H NMR ([D_6]-DMSO): δ = 6.45–6.51, 6.60–6.70, and 7.16–7.25 (3 m, 3 H, 20-Ph-*m*,*p*-H); 7.81–7.86 (m, 9 H, 5,10,15-Ph-*m*,*p*-H); 8.09–8.27 (m, 13H, 2 20-Ph-*o*-H, 4 Ph-*o*-H and Pc-β-H); 8.38–8.46 (m, 2 H, Ph-*o*-H); 8.70 and 8.75 (2 d, J = 4.7 Hz, 2 H, Por-β-H); 8.82 (AB, J = 4.8 Hz, 2 H, Por-β-H); 8.87 (AB, J = 4.8 Hz, 2 H, Por-β-H); 9.05 (d, J = 7.8 Hz, 1 H, 4′-H); 9.18 (s, 1 H, 3-H); 9.30–9.40 (m, 7 H, Pc-α-H) ppm. ^{13}C NMR ([D_6]DMSO): δ = 120.2; 120.4; 120.8; 121.3 (C-4′); 121.9, 122.5, and 122.8 (Pc-α-C); 123.8 (C-1′); 126.8, 127.6, and 127.7 (Ph-*m*,*p*-C); 128.9, 129.60, 129.66 and 129.72 (Pc-β-C); 131.4, 131.9, 132.0, and 132.5 (Por-β-C and C-3′); 134.3 (Ph-*o*-C); 135.3 (C-3); 137.3; 137.92; 137.95; 140.9; 141.7; 142.7; 143.0; 146.2; 147.0; 147.05; 149.5; 149.6; 149.7; 150.6; 152.8; 152.9; 153.0; 153.06; 153.1; 153.5 ppm. UV/Vis (THF): λ_{max} (log ε) = 344 (4.7),

425 (5.5), 560 (4.1), 608 (4.5), 673 (5.4) nm. HRMS (MALDI-TOF): *m*/*z* = 1250.2258 (calcd. 1250.2238).

Triad 1: UV/Vis (THF): λ_{max} (%) = 425 (100), 559 (5.8), 614 (7.7), 680 (41) nm. HRMS (MALDI-TOF): *m*/*z* = 1924.3629 (calcd. 1924.3682).

Dyad 2: Yield: 14.5 mg (21%); m.p. > 300 °C. ^{1}H NMR ($CDCl_3$): δ = 1.18–1.37 (m, 18 H, CH_3), 1.78–1.98 (m, 12 H, CH_2CH_3), 2.12–2.34 (m, 12 H, $CH_2CH_2CH_3$), 3.99–4.17 (m, 3 H, OCH_2), 4.40–4.83 (m, 9 H, OCH_2), 5.61 (t, *J* = 7.3 Hz 1 H, 20-Ph-*m*-H), 6.00 (d, *J* = 7.5 Hz, 1 H, 20-Ph-*o*-H), 6.07–6.13 (m, 2 H, 20-Ph-*m*,*p*-H), 7.08 (d, *J* = 7.5 Hz, 1 H, Ph-*o*-H), 7.51 (t, *J* = 7.5 Hz, 1 H, Ph-*m*-H), 7.64 (d, *J* = 4.6 Hz, 1 H, Por-β-H), 7.72–8.01 (m, 10 H, 2 β-H, 2 Ph-*o*-H, 5 Ph-*m*,*p*-H, 4′-H), 7.91 (s, 1 H, 1′-H), 8.28–8.44 (m, 5 H, 3 β-H and 2 Ph-*m*-H), 8.43, 8.55, 8.90, 8.94 and 9.02 (5 s, 5 H, Pc-α-H), 8.50 (t, *J* = 7.7 Hz, 1 H, Ph-*m*-H), 8.69 (d, *J* = 7.5 Hz, 1 H, 20-Ph-*o*-H), 9.27 (d, *J* = 7.7 Hz, 1 H, 3′-H), 10.31 (d, *J* = 7.7 Hz, 1 H, Ph-*o*-H), 10.37 (s, 1 H, 25′-H), 10.45 (d, *J* = 7.5 Hz, 1 H, Ph-*o*-H), 10.53 (s, 1 H, 3-H), 10.70 (d, *J* = 7.3 Hz, 1 H, Ph-*o*-H) ppm. ^{13}C NMR ($CDCl_3$): δ = 14.17, 14.21, 14.27, and 14.32 (CH_3); 19.53, 19.59, 19.60, 19.61, and 19.66 (CH_2CH_3); 31.6 and 31.8 ($CH_2CH_2CH_3$); 68.5, 69.2, 69.3, and 69.5 (OCH_2); 105.36, 105.43, 105.7, 105.8, and 106.2 (Pc-α-C); 106.9 (C-25′); 117.4, 119.2, 119.9, 120.33, and 120.37 (C-3′); 123.8, 125.1, 125.5, 125.8, 125.9, 126.0, 126.2, 126.5, 126.7, 126.9, 127.0, and 127.5 (Ph-*m*,*p*-H); 129.8, 129.9, 130.0, 131.2, and 131.3 (Por-β-C); 130.4 (C-3); 130.6, 131.0, 131.2, 131.5, and 133.0 (C-1′); 133.2, 133.3, 134.8, 135.0, 136.1, 136.2, and 136.9 (Ph-*o*-C); 134.4; 136.5; 138.7; 141.0; 142.6; 143.8; 143.9; 144.9; 145.6; 146.2; 148.1; 148.6; 148.9; 149.0; 149.1; 149.4; 150.3; 150.5; 150.6; 150.8; 150.99; 151.0; 151.2; 151.5; 151.6; 151.8; 152.6 ppm. UV/Vis (THF): λ_{max} (log ε) = 355 nm (4.9), 425 (5.6), 560 (4.1), 611 (4.5), 677 (5.4). HRMS (MALDI-TOF): *m*/*z* = 1682.5652 (calcd. 1682.5689).

Triad 2: UV/Vis (THF): λ_{max} (%) = 425 (100), 560 (6.4), 616 (7.1), 683 (34) nm. HRMS (MALDI-TOF): *m*/*z* = 2212.5945 (calcd. 2212.5982).

Dyad 3: Yield: 15 mg (26%); m.p. > 300 °C. UV/Vis (THF): λ_{max} (log ε) = 348 (4.9), 425 (5.6), 560 (4.2), 611 (4.6), 677 (5.4) nm. HRMS (MALDI-TOF): *m*/*z* = 1418.4134 (calcd. 1418.4116).

Triad 3: UV/Vis (THF): λ_{max} (%) = 426 (100), 559 (5.8), 615 (6.0), 683 (31) nm. HRMS (MALDI-TOF): *m*/*z* = 2036.4962 (calcd. 2036.4934).

Porphyrin–Phthalonitrile 4: A stirred mixture of **6** (50 mg, 67 μmol) and DDQ (140 mg, 62 μmol) in toluene (6 mL) was heated at reflux for 24 h. The reaction mixture was filtered through a short plug of Celite, washed with an aqueous $NaHCO_3$ solution, dried (Na_2SO_4), and the solvent removed under reduced pressure. The residue was taken up in CH_2Cl_2 and purified by flash chromatography (silica gel) using toluene as eluent. Some starting porphyrin (5.3 mg, 11%) and the expected derivative **4** (37.8 mg, 85% yield based on the consumed **6**) were obtained; both compounds were crystallized from CH_2Cl_2/petroleum ether; m.p. > 300 °C. ^{1}H NMR ($CDCl_3$): δ = –2.65 (s, 2 H, NH), 7.35 (t, *J* = 7.2 Hz, 2 H, 20-Ph-*m*-H), 7.39–7.46 (m, 1 H, 20-Ph-*p*-H), 7.47 (d, *J* = 8.4 Hz, 1 H, 3′-H), 7.63–7.67 (m, 2 H, 2′-H and 6′-H), 7.70–7.80 (m, 9 H, Ph-*m*,*p*-H), 7.90 (d, *J* = 6.9 Hz, 2 H, Ph-*o*-H), 8.18–8.23 (m, 6 H, Ph-*o*-H), 8.72 (s, 1 H, 3-H), 8.77–8.80 (m, 3 H, β-H), 8.83 (d, *J* = 4.9 Hz, 1 H, β-H), 8.87 and 8.90 (AB, *J* = 4.9 Hz, 2 H, β-H) ppm. ^{13}C NMR ($CDCl_3$): δ = 111.9, 114.5, 115.4, 115.8, 120.2, 120.5, 120.6, 120.8, 126.7, 126.8, 126.9, 127.9, 128.0, 128.2, 129.8, 130.3, 132.2, 133.0, 133.3, 133.8, 134.5, 134.6, 135.0, 136.1, 140.4, 141.5, 141.8, 142.0, 145.0 ppm. UV/Vis (THF): λ_{max} (log ε) = 421 (5.5), 517 (4.2), 552 (3.8), 596 (3.6), 652 (3.5) nm. HRMS (MALDI-TOF): *m*/*z* = 740.2267 (calcd. 740.2683).

2-(Buta-1,3-dien-2-yl)-5,10,15,20-tetraphenylporphyrin (5): An *o*-dichlorobenzene (30 mL) solution of porphyrin **13** (140 mg, 192 μmol) and DBU (1 mL, 7 μmol) was refluxed for 30 min. The mixture was cooled to room temperature and was then submitted to column chromatography (silica gel) with petroleum ether to remove the *o*-dichlorobenzene and then a mixture of petroleum ether and toluene (1:1) to elute **5**. Evaporation of the solvent followed by crystallization from CH_2Cl_2/MeOH afforded pure **5** (111 mg, 87% yield); m.p. > 300 °C. ^{1}H NMR ($CDCl_3$): δ = –2.70 (s, 2 H, NH), 4.61 (d, *J* = 17.2 Hz, 1 H, 3′-*trans*-H), 4.92 (d, *J* = 10.5 Hz, 1 H, 3′-*cis*-H), 5.12 and 5.19 (2 br. s, 2 H, 4′-H), 6.41 (dd, *J* = 10.5 and 17.2 Hz, 1 H, 2′-H), 7.47 (t, *J* = 7.7 Hz, 2 H, 20-Ph-*m*-H), 7.63 (t, *J* = 7.7 Hz, 1 H, 20-Ph-*p*-H), 7.68–7.76 (m, 9 H, Ph-*m*,*p*-H), 7.96 (d, *J* = 7.7 Hz, 2 H, 20-Ph-*o*-H), 8.19–8.23 (m, 6 H, Ph-*o*-H), 8.65 (s, 1 H, 3–H), 8.70 and 8.76 (2 d, *J* = 4.8 Hz, 2 H, β-H), 8.80–8.84 (m, 4 H, β-H) ppm. ^{13}C NMR ($CDCl_3$): δ = 116.4, 119.7, 120.0, 120.3, 120.6, 120.9, 125.7, 126.63, 126.64, 126.7, 127.6, 127.65, 127.7, 130.7–131.9 (C-β) 134.5, 134.6, 135.9, 141.0, 141.4, 141.9, 142.3, 142.4, 143.6 ppm. UV/Vis (THF): λ_{max} (%) = 417 (100), 514 (4.8), 548 (1.7), 592 (1.3), 648 (0.7) nm. HRMS (MALDI-TOF): *m*/*z* = 666.2789 (calcd. 666.2783).

Compound 6: A toluene (12 mL) solution of **5** (60 mg, 90 μmol) and 1,2-dicyanoethylene (80 mg, 1 mmol) was refluxed overnight. The reaction mixture was concentrated and submitted to column chromatography (silica gel) with a mixture of petroleum ether and toluene (1:1) as eluent. Compound **6** (59 mg, 88% yield) was crystallized from CH_2Cl_2/MeOH; m.p. > 300 °C. ^{1}H NMR ($CDCl_3$): δ = –2.74 (s, 2 H, NH), 2.24–2.33 (m, 2 H, 4′,5′-H), 2.50–2.97 (m, 4 H, 3′,6′-H), 5.64 (br. s, 1 H, 2′-H), 7.69–7.81 (m, 12 H, Ph-*m*,*p*-H), 8.10–8.19 (m, 8 H, Ph-*o*-H), 8.54 (s, 1 H, 3-H), 8.63 (d, *J* = 4.9 Hz, 1 H, β-H), 8.79 (d, *J* = 4.9 Hz, 1 H, β-H), 8.81–8.82 (m, 3 H, β-H), 8.85 (d, *J* = 4.9 Hz, 1 H, β-H) ppm. ^{13}C NMR ($CDCl_3$): δ = 28.1, 28.8, 29.0, 34.1, 118.7, 119.1, 119.5, 119.9, 120.4, 120.6, 125.4, 126.4, 126.7, 126.8, 127.8, 127.9, 128.0, 130.5–131.9 (C-β), 132.6, 134.5, 134.6, 135.0, 136.2, 141.6, 142.0, 142.1, 142.2 ppm. UV/Vis (THF): λ_{max} (%) = 418 (100), 515 (5.0), 549 (1.8), 593 (1.3), 649 (0.8) nm. HRMS (MALDI-TOF): *m*/*z* = 744.3025 (calcd. 744.3001).

(2-Nitro-5,10,15,20-tetraphenylporphyrinato)copper(II) (7): $Cu(NO_3)_2 \cdot 3H_2O$ (500 mg, 2.1 mmol) dissolved in a mixture of acetic anhydride (50 mL) and acetic acid (10 mL) was added to a $CHCl_3$ (500 mL) solution of TPP (500 mg, 814 μmol). The mixture was stirred at 40 °C until almost complete conversion of the starting porphyrin (ca. 32 h). The solvents were then evaporated to dryness and the residue was dissolved in CH_2Cl_2 and submitted to chromatography (a short plug of silica gel) with toluene/petroleum ether (2:1) as eluent. The 2-nitro-TPP **7** was crystallized from CH_2Cl_2/petroleum ether (520 mg, 89% yield). The compound is identical (TLC, UV/Vis and MS) with an authentic sample prepared previously.[17]

(2-Amino-5,10,15,20-tetraphenylporphyrinato)copper(II) (8): Tin powder (2.8 g) and then concentrated HCl (9 mL) were added to a solution of **7** (200 mg, 277 μmol) in $CHCl_3$ (20 mL). The reaction mixture was sonicated in an ultrasonic bath for 1 h. The mixture was then filtered through a short plug of Celite, neutralized with $NaHCO_3$, washed with water, extracted with $CHCl_3$, and the combined organic layers dried (Na_2SO_4). The solvent was evaporated and the residue was submitted to column chromatography (silica gel) with toluene/petroleum ether as eluent. Porphyrin **8** was crystallized from CH_2Cl_2/petroleum ether (152 mg, 79% yield). The

compound is identical (TLC, UV/Vis and MS) with an authentic sample prepared previously.[17]

Compound 10: Concentrated H_2SO_4 (0.76 mL) was added dropwise to a mixture of **8** (250 mg, 0.36 mmol) and sodium nitrite (30 mg, 0.43 mmol) in THF containing 1% H_2O (75 mL). The mixture was stirred at room temperature until a change of color from violet to green was observed (ca. 45 min); the TLC of the mixture showed a very polar green spot. Then, palladium acetate (30 mg, 0.13 mmol) and 3-sulfolene (367 mg, 3.11 mmol) were added and the reaction mixture was stirred at 65 °C for 1 h (the color changed from green to red). The reaction mixture was cooled to room temperature and then filtered through a short plug of Celite, neutralized with an aqueous solution of Na_2CO_3, washed with water, extracted with CH_2Cl_2, and dried (Na_2SO_4). The solvent was evaporated and the residue was purified by flash chromatography with a mixture of $CHCl_3$ and petroleum ether (1:1) as eluent to afford compound **10** (230 mg, 81% yield); m.p. > 300 °C. UV/Vis (THF): λ_{max} (%) = 416 (100), 541 (4), 581 (1) nm. HRMS (MALDI-TOF): *m*/*z* = 791.1545 (calcd. 791.1536).

Compound 13. a) From 10: Concentrated H_2SO_4 (5 mL) was added dropwise to a vigorously stirred solution of porphyrin **10** (100 mg, 126 μmol) in $CHCl_3$ (100 mL) at room temperature. After about 2–3 min, the reaction mixture was neutralized with dilute aqueous Na_2CO_3, washed with water, extracted with CH_2Cl_2, and dried (Na_2SO_4). The solvent was removed and the residue was submitted to column chromatography (silica gel) with CH_2Cl_2 as eluent. Compound **13** was crystallized from CH_2Cl_2/petroleum ether (85 mg, 92% yield). **b) From 12:** TFA (1 mL) was added dropwise to a vigorously stirred solution of porphyrin **12** (12 mg, 15 μmol) in $CHCl_3$ (5 mL) at room temperature. After about 2–3 min, the reaction mixture was neutralized with dilute aqueous Na_2CO_3, washed with water, extracted with CH_2Cl_2, and dried (Na_2SO_4). Compound **13** was crystallized from CH_2Cl_2/petroleum ether (10.5 mg, 96% yield); m.p. > 300 °C. ^{1}H NMR ($CDCl_3$): δ = –2.76 (s, 2 H, NH), 3.29–3.44 (m, 2 H, 5′-H), 4.58–4.62 (m, 2 H, 1′-H), 6.73 (dd, *J* = 2.3 and 6.6 Hz, 1 H, 3′-H), 6.96 (dd, *J* = 3.0 and 6.6 Hz, 1 H, 2′-H), 7.71–7.87 (m, 12 H, Ph-*m*,*p*-H), 8.11–8.21 (m, 8 H, Ph-*o*-H), 8.61 (s, 1 H, 3-H), 8.64 (d, *J* = 4.9 Hz, 1 H, β-H), 8.79–8.82 (m, 4 H, β-H), 8.85 (d, *J* = 4.9 Hz, 1 H, β-H) ppm. ^{13}C NMR ($CDCl_3$): δ = 39.3 (C-1′), 57.2 (C-5′), 118.8, 120.2, 120.5, 120.7, 124.5, 126.6, 126.7, 126.8, 126.9, 127.3, 127.4, 127.8, 128.0, 129.2, 130.0–132.5 (C-β), 130.9, 133.2, 133.9, 134.5, 134.6, 141.6, 141.92, 141.94, 142.5 ppm. UV/Vis (THF): λ_{max} (%) = 418 (100), 514 (4.6), 548 (1.6), 592 (1.2), 648 (0.7) nm. HRMS (MALDI-TOF): *m*/*z* = 730.2400 (calcd. 730.2402).

(2-Bromo-5,10,15,20-tetraphenylporphyrinato)zinc(II) (11b): This compound was synthesized by a known procedure.[20] A mixture of TPP (200 mg, 326 μmol) and *N*-bromosuccinimide (102 mg, 573 μmol) in $CHCl_3$ (50 mL) was stirred at room temperature for 6 h. The solvent was evaporated and the mixture was washed with water, extracted with $CHCl_3$, dried (Na_2SO_4), and the solvent evaporated. The residue was purified by column chromatography with a mixture of petroleum ether, toluene, and dichloromethane (2:1.4:0.6) as eluent. The first (44.3 mg, 18% yield) and third fractions (89.7 mg, 39% yield) to be collected were identified by mass spectrometry and ^{1}H NMR spectroscopy as mixtures of β,β′-dibromoporphyrins. The second fraction contained the desired β-monobromoporphyrin **11a** (35.5 mg, 16% yield). UV/Vis (THF): λ_{max} (%) = 420 (100), 519 (6), 596 (2), 657 (2) nm. ^{1}H NMR ($CDCl_3$): δ = –2.85 (s, 2 H, NH), 7.68–7.80 (m, 12 H, Ph-*m*,*p*-H), 8.07–8.10 (m, 2 H, 20-Ph-*o*-H), 8.17–8.22 (m, 6 H, Ph-*o*-H), 8.76 (AB, *J* = 4.9 Hz, 2 H, 12-H and 13-H), 8.81 and 8.85 (AB, *J* = 5.0 Hz, 2 H, β-H), 8.87 (s, 1 H, 3-H), 8.88 and 8.90 (AB, *J* = 4.9 Hz, 2 H, β-H) ppm. MS (FAB$^+$): *m*/*z* = 694 [M + H]$^+$. A solution of **11a** (20 mg, 29 μmol) in a mixture of $CHCl_3$ and MeOH (2:1) (5 mL) was stirred with an excess of zinc acetate dihydrate (13 mg, 59 μmol, 2 equiv.) at 65 °C. After 20 min, the reaction mixture was washed with water and the organic layer was dried (Na_2SO_4). Compound **11b** was crystallized from CH_2Cl_2 and petroleum ether (21.5 mg, 98% yield); m.p. > 300 °C. UV/Vis (THF): λ_{max} (%) = 425 (100), 557 (4), 596 (1) nm.

Compound 12: 3-Sulfolene (406 mg, 3.44 mmol), palladium acetate (3.3 mg, 15 μmol), triphenylphosphane (7.8 mg, 30 μmol), and sodium acetate (45.6 mg, 0.56 mmol) were added to a solution of **11b** (20 mg, 26 μmol) in DMF (5 mL). The mixture was refluxed under nitrogen for 24 h. Water and diethyl ether were then added and the organic layer was separated and dried (Na_2SO_4). The solvent was evaporated, the crude residue was dissolved in toluene and submitted to column chromatography (silica gel) with a gradient of petroleum ether/toluene (1:1) and CH_2Cl_2 as eluent. The first fraction to be collected was identified as the expected porphyrin **12** (6.2 mg, 49% yield based on the consumed **11b**). The second fraction was the starting porphyrin **11b** (8 mg, 40%); m.p. > 300 °C. ^{1}H NMR ($CDCl_3$): δ = 3.37–3.47 (m, 2 H, 5′-H), 4.63–4.68 (m, 1 H, 1′-H), 6.74 (dd, *J* = 2.3 and 6.6 Hz, 1 H, 3′-H), 7.02 (dd, *J* = 2.9 and 6.6 Hz, 1 H, 2′-H), 7.71–7.85 (m, 12 H, Ph-*m*,*p*-H), 8.11–8.21 (m, 8 H, Ph-*o*-H), 8.70 (d, *J* = 4.8 Hz, 1 H, β-H), 8.76 (s, 1 H, 3-H), 8.88–8.95 (m, 5 H, β-H) ppm. UV/Vis (THF): λ_{max} (%) = 424 (100), 557 (4), 596 (1) nm. HRMS (MALDI-TOF): *m*/*z* = 792.1541 (calcd. 792.1532).

Photophysics: Femtosecond transient-absorption studies were performed with 387-nm laser pulses (1 kHz, 150-fs pulse width) from an amplified Ti:Sapphire laser system (Clark-MXR, Inc.). Nanosecond Laser Flash Photolysis experiments were performed with laser pulses from a Quanta-Ray CDR Nd:YAG system (532 nm, 6-ns pulse width) in a front-face excitation geometry. Fluorescence lifetimes were measured with a Laser Strope Fluorescence Lifetime Spectrometer (Photon Technology International) with 337-nm laser pulses from a nitrogen laser fiber-coupled to a lens-based T-formal sample compartment equipped with a stroboscopic detector. Details of the Laser Strobe systems are described on the manufacture's web site (http://www.pti-nj.com). Emission spectra were recorded with an SLM 8100 Spectrofluorometer. The experiments were performed at room temperature. Each spectrum represents an average of at least five individual scans, and appropriate corrections were applied whenever necessary. The UV/Vis spectra of dyad **1** and triads **1**–**3**, the ^{1}H NMR spectrum of dyad **1** in [D_6]DMSO, COSY and HSQC NMR spectra of dyads **1** and **2**, and the differential absorption spectrum obtained upon femtosecond flash photolysis of a solution of ZnTPP in toluene with several time delays are collected in the Supporting Information.

Acknowledgments

This work was carried out with partial support from the Fundação para a Ciência e a Tecnologia (FCT), Portugal (project POCTI/1999/QUI/32851), the Ministerio de Educación y Ciencia (CTQ-2005-08933-BQU), the Comunidad de Madrid, Spain (GR/MAT/0513/2004), the EU (RTN networks "WONDERFULL" and "CASSIUSCLAYS"), the Deutsche Forschungsgemeinschaft (SFB 583), and the Office of Basic Energy Sciences of the U.S. Department of Energy. This is document NDRL-4444 from the Notre Dame Radiation Laboratory. J. P. C. T. and C. M. A. A. are also grateful to FCT for their postdoctoral grants.

[1] I. Rosenthal, in *Phthalocyanines − Properties and Applications* (Eds.: C. C. Leznoff, A. B. P. Lever), VCH, New York, **1996**, vol. 4, chapter 13.
[2] E. Ben-Hur, W.-S. Chan, in *The Porphyrin Handbook* (Eds.: K. M. Kadish, K. M. Smith, R. Guilard), Academic Press, New York, **2003**, vol. 19, chapter 117.
[3] D. Wohrle, O. Suvorova, R. Gerdes, O. Bartels, L. Lapok, N. Baziakina, S. Makarov, A. Slodek, *J. Porphyrins Phthalocyanines* **2004**, *8*, 1020.
[4] M. Kimura, H. Shirai, in *The Porphyrin Handbook* (Eds.: K. M. Kadish, K. M. Smith, R. Guilard), Academic Press, New York, **2003**, vol. 19, chapter 120.
[5] N. B. McKeown, *Phthalocyanine Materials: Synthesis, Structure and Function*, Cambridge University Press, Cambridge, **1998**.
[6] a) G. de la Torre, P. Vázquez, F. Agulló-López, T. Torres, *J. Mater. Chem.* **1998**, *8*, 1671; b) G. de la Torre, P. Vázquez, F. Agulló-López, T. Torres, *Chem. Rev.* **2004**, *104*, 3723.
[7] a) D. Dini, M. Hanack, *J. Porphyrins Phthalocyanines* **2004**, *8*, 915; b) D. Dini, M. Hanack, in *The Porphyrin Handbook* (Eds.: K. M. Kadish, K. M. Smith, R. Guilard), Academic Press, New York, **2003**, vol. 16, chapter 107.
[8] a) M. R. Wasielewski, *Chem. Rev.* **1992**, *92*, 435; b) D. Gust, T. A. Moore, A. L. Moore, *Acc. Chem. Res.* **2001**, *34*, 40; c) D. M. Guldi, *Pure Appl. Chem.* **2003**, *75*, 1069; d) H. Imahori, Y. Mori, Y. L. Matano, *Photochem. Photobiol.* **2003**, *4*, 51; e) D. Wöhrle, D. Meissner, *Adv. Mater.* **1991**, *3*, 129; f) M. A. Loi, P. Denk, H. Hoppe, H. Neugebauer, C. Winder, D. Meissner, C.-J. Brabec, N. S. Sariciftci, A. Gouloumis, P. Vázquez, T. Torres, *J. Mater. Chem.* **2003**, *13*, 700.
[9] a) A. Gouloumis, S.-G. Liu, A. Sastre, P. Vázquez, L. Echegoyen, T. Torres, *Chem. Eur. J.* **2000**, *6*, 3600; b) A. Gouloumis, S.-G. Liu, P. Vázquez, L. Echegoyen, T. Torres, *Chem. Commun.* **2001**, 399; c) D. M. Guldi, J. Ramey, M. V. Martínez-Díaz, A. de la Escosura, T. Torres, T. Da Ros, M. Prato, *Chem. Commun.* **2002**, 2774; d) A. González-Cabello, P. Vázquez, T. Torres, D. M. Guldi, *J. Org. Chem.* **2003**, *68*, 8635; e) H. Li, J. O. Jeppesen, E. Levillain, J. Becher, *Chem. Commun.* **2003**, 846; f) D. González-Rodríguez, T. Torres, M. A. Herranz, J. Rivera, L. Echegoyen, D. M. Guldi, *J. Am. Chem. Soc.* **2004**, *126*, 6301; g) J. L. Sessler, J. Jayawickramarajah, A. Gouloumis, T. Torres, D. M. Guldi, S. Maldonado, K. J. Stevenson, *Chem. Commun.* **2005**, 1892.
[10] a) E. M. Maya, P. Vázquez, T. Torres, *Chem. Eur. J.* **1999**, *5*, 2004; b) A. de la Escosura, M. V. Martínez-Díaz, P. Thordarson, A. E. Rowan, R. J. M. Nolte, T. Torres, *J. Am. Chem. Soc.* **2003**, *125*, 12300.
[11] G. de la Torre, M. V. Martínez-Díaz, P. A. Ashton, T. Torres, *J. Org. Chem.* **1998**, *63*, 8888.
[12] D. González-Rodríguez, C. G. Claessens, *Chem. Eur. J.*, in press.
[13] a) N. Kobayashi, Y. Nishiyama, T. Ohya, M. Sato, *J. Chem. Soc., Chem. Commun.* **1987**, 390–392; b) H.-J. Tian, Q.-F. Zhou, S.-Y. Shen, H.-J. Xu, *J. Photochem. Photobiol. A* **1993**, *72*, 163; c) H.-J. Tian, Q.-F. Zhou, S.-Y. Shen, H.-J. Xu, *Chin. J. Chem.* **1996**, *14*, 412; d) H.-J. Tian, Q.-F. Zhou, S.-Y. Shen, H.-J. Xu, *Chin. J. Chem.* **1998**, *16*, 97.
[14] a) S. I. Yang, J. Li, H. S. Cho, D. Kim, D. F. Bocian, D. Holten, J. S. Lindsey, *J. Mater. Chem.* **2000**, *10*, 283; b) A. Ambroise, R. W. Wagner, P. D. Rao, J. A. Riggs, P. Hascoat, J. R. Diers, J. Seth, R. K. Lammi, D. F. Bocian, D. Holten, J. S. Lindsey, *Chem. Mater.* **2001**, *13*, 1023; c) M. A. Miller, R. K. Lammi, S. Prathapan, D. Holten, J. S. Lindsey, *J. Org. Chem.* **2000**, *65*, 6634; d) J. M. Sutton, R. W. Boyle, *Chem. Commun.* **2001**, 2014.
[15] K. Kameyama, A. Satake, Y. Kobuke, *Tetrahedron Lett.* **2004**, *45*, 7617.
[16] C. M. A. Alonso, M. G. P. M. S. Neves, A. C. Tomé, A. M. S. Silva, J. A. S. Cavaleiro, *Tetrahedron Lett.* **2000**, *41*, 5679.
[17] H. K. Hombrecher, V. M. Gherdan, S. Ohm, J. A. S. Cavaleiro, M. G. P. M. S. Neves, M. F. Condesso, *Tetrahedron* **1993**, *49*, 8569.
[18] Taking into account the large red-shifts observed in the Q-band of phthalocyanine- and subphthalocyanine-fused dimers wherein the chromophores are fully π-conjugated and forced to be planar with respect to each other (see: G. de la Torre, M. V. Martínez-Díaz, P. R. Ashton, T. Torres, *J. Org. Chem.* **1998**, *63*, 8888; C. G. Claessens, T. Torres, *Angew. Chem. Int. Ed.* **2002**, *41*, 2561), the dyads reported herein may adopt an orthogonal or pseudo-orthogonal geometry, which additionally avoids steric hindrance between the *meso*-phenyl groups and the phthalocyanine moiety, rather than a planar arrangement of the porphyrin and phthalocyanine rings.
[19] S. L. Murov, I. Carmichael, G. L. Hug, *Handbook of Photochemistry*, Marcel Dekker Inc., New York, **1993**.
[20] a) H. J. Callot, *Tetrahedron Lett.* **1973**, *14*, 4987; b) M. J. Callot, *Bull. Soc. Chim. Fr.* **1974**, 1492.

Received: July 22, 2005
Published Online: November 10, 2005

